Megascale rhythmic shoreline forms on a beach with multiple bars*

OCEANOLOGIA, 50 (2), 2008.
pp. 183–203.

KEYWORDS
Mega-cusps
Multibar profile
Bars
Baltic Sea
nearshore zone

Zbigniew Pruszak*
Grzegorz Różyński
Piotr Szmytkiewicz

Institute of Hydroengineering,
Polish Academy of Sciences,
(IBW PAN),
Kościerska 7, PL–80–328 Gdańsk, Poland;

e-mail: zbig@ibwpan.gda.pl

*corresponding author

Received 27 December 2007, revised 10 April 2008, accepted 19 May 2008.

Abstract

The study, carried out in 2003 and 2006 at the Lubiatowo Coastal Research Station (Poland), located on the non-tidal southern Baltic coast (tidal range < 0.06 m), focused on larger rhythmic forms (mega-cusps) with wavelengths in the interval 500 m $> L_c >$ 20 m. Statistical analyses of detailed shoreline configurations were performed mostly with the Discrete Wavelet Transform method (DWT). The beach is composed of fine sand with grain diameter $D_{50} \approx 0.22$ mm, which produces 4 longshore sandbars and a gently sloping seabed with $\beta = 0.015$. The analysis confirms the key role of bars in hydro- and morphodynamic surf zone processes.

* The paper presents results of the research carried out within the project N306 003 31/0081 entitled: 'Determination and description of relationships between sediment motion, flow structures and bottom changes, together with extension and verification of the model of these phenomena for shallow water areas of a multi-bar (dissipative) and a non-bar (reflective) shore', funded by the Ministry of Science and Higher Education (Poland).

The hypothesis was therefore set up that, in a surf zone with multiple bars, the bars and mega-scale shoreline rhythmic forms form one integrated physical system; experimental evidence to substantiate this hypothesis was also sought. In such a system not only do self-regulation processes include swash zone phenomena, they also incorporate processes in offshore surf zone locations. The longshore dimensions of large cusps are thus related to the distances between periodically active large bed forms (bars). The spatial dimension of bar system activity (number of active bars) depends, at a given time scale, on the associated hydrodynamic conditions. It was assumed that such a time scale could include either the development and duration of a storm, or a period of stable, yet distinct waves, capable of remodelling the beach configuration. The indentation to wavelength ratio of mega-cusps for the studied non-tidal dissipative environment may be one order of magnitude greater than for mesotidal, reflective beaches.

1. Introduction

Among a number of morphological shoreline forms, rhythmic undulations featuring alternating, clearly visible horns and gentle embayments have been accorded particular attention over a number of years. These features, collectively known as beach cusps, can be of various scales (e.g. Guza & Inman 1975, Komar 1998, Nolan et al. 1999, Sunamura 2004). In some cases large rhythmic shoreline forms are referred to as longshore sand waves, although the latter should really be classified among shoreline features, whose properties differ somewhat from those of beach cusps. One of the differences is the considerable longshore mobility of sand waves and their greater affinity for longshore sediment transport. The current study concentrates on rhythmic shoreline forms which, though subject to local transformations, do not undergo longshore migration. Such morphological forms are rhythmic shoreline undulations known as beach cusps (mega-cusps).

Since individual cusps (mega-cups) can vary in size from several to many hundreds of metres, knowledge of their dimensions and range of variability is an interesting aspect of coastal engineering. Due to their fairly regular, rhythmic shape and spatial repeatability, comparable with certain infragravity waves (edge waves), numerous relationships exist between these two phenomena (e.g. Guza & Inman 1975, Komar 1998, Ruessink 1998). Apart from the relations between infragravity waves and rhythmic shoreline forms, another idea that focuses on shallow-water self-organising processes as major drivers of beach cusp formation is currently gaining popularity (Werner & Fink 1993, Coco et al. 1999, 2001). In this context self-regulatory processes are understood as dynamic interactions of various morphological shoreline features with longshore-variable wave-current structures that form in the swash zone in direct proximity to the shoreline.

Extensive field observations of ocean shores, consisting of sediments varying from fine sand ($D = 0.25$ mm) to gravel ($D = 32$ mm) (Nolan et al. 1999) have indicated that the average longshore dimension of a single cusp varies between 2.95 and 87.5 m, whereas the average indentation length (the horizontal depth-term used by Nolan et al. (1999)) of such undulations, i.e. the distance between the tips of a horn and the hollow, varies between 2.5 and 41 m. Other studies and research results also indicate the presence of certain proportions between the geometries of a single feature (see e.g. Komar 1998). The empirical formula obtained by Nolan et al. (1999) relating the cusp length L_c to its indentation length A_c is

$$L_c = 2.2A_c \quad [\text{m}]. \tag{1}$$

From this equation it can be deduced that rhythmic ocean shore forms cut deep into beaches, reaching up to about 50% of the cusp length. On the basis of available measurements of beach cusp spacing, Sunamura (2004) presented an empirical relationship linking cusp length with wave parameters and sediment diameter as follows:

$$L_c = K\phi T\sqrt{gH} \quad [\text{m}], \tag{2}$$

where T and H respectively stand for the wave period and wave height in a shallow-water area, K is a dimensionless empirical parameter equal to 1.35, and parameter $\phi = \exp(-0.23D^{0.55})$. The quantity D in the equation for ϕ expresses the sediment grain diameter in [mm]. This eq. (2) has been discussed in relation to various laboratory and field datasets. For the field data the beach cusp lengths varied from several to several tens of metres (maximum $L_c = 66.6$ m). The sediment grain diameter varied from $D = 0.2$ mm (one case) to $D = 14$ mm, and the height and period of waves lay between $H = 0.3$–1.88 m and $T = 4$–16 s. In the majority of datasets used by Sunamura the length L_c was equal to about ten metres.

On the assumption that self-organising processes in the swash zone are the major drivers of beach cusp formation, Werner & Fink (1993) proposed a simple relationship between cusp length L_c and the swash process (swash excursion l_S):

$$L_c = kl_S, \tag{3}$$

where k can vary from 1.5 to 1.7, depending on various research results.

Long-term observations of longshore undulations along a section of the southern Baltic coast point to the existence of a fairly large number of multi-scale shoreline forms. However, even a superficial assessment of these observations reveals the inherent instability and considerable geometric differentiation of such forms. In addition, the geometry and regularity of different-scale beach cusps are less conspicuous than those present

on reflective ocean shores. For the dissipative southern Baltic coast the longshore dimension of a single undulation usually varies between several tens and several hundreds of metres with a cross-shore amplitude of between several tens of centimetres to several metres at most (Pruszak et al. 2007). The rhythmic shoreline forms can mostly be seen during a period of relative calm after a storm.

The majority of analyses and studies on the identification, geometric characteristics and evolution of beach cusps (mega-cusps) have so far focused on ocean shores without bars or with a very limited number of bars. These shores are mostly reflective, where a single breaker occurs near the shoreline and where considerable wave reflection is present. Hence, we can assume that there are considerable differences or additional factors in the formation and evolution of shoreline rhythmicity in multi-bar, dissipative shores of shelf seas, e.g. the Baltic Sea, in contrast to reflective ocean beaches. In addition, tidal action on the beaches of shelf seas is usually negligible, owing to their isolation from large water bodies such as the Atlantic Ocean.

On the basis of some classical studies by Wright & Short (1984), the detailed analyses given by e.g. Coco et al. (1999) and Werner & Fink (1993) and the present authors' long-term field observations and studies, we put forward the hypothesis that the formation and geometric characteristics of larger rhythmic shoreline forms result from larger-scale self-organising processes, encompassing most of the surf zone width, shaping nearshore morphology. On dissipative beaches with multiple bars the key role is played by well-pronounced bars, which influence shoreline dynamics and evolution. The existing physical interactions and correlations between the nearshore bars (mainly two inner bars) and shoreline position (Pruszak et al. 1997, 1999) is a strong argument in favour of this way of thinking. The question therefore arises to what extent different physical conditions are responsible for the different character and parameters of large beach cusps generated on dissipative shores. Assuming that the nearshore bar system is the key element of surf zone hydro- and morphodynamics, the aim of this paper is to discuss and attempt to test experimentally the above hypothesis relating the longshore dimensions of large shoreline rhythmic forms with instantaneously active bars and their offshore distances. In limiting the research to mega-cusps, both smaller cusps ($L_c < 20$ m) and giant ones ($L_c > 500$ m) were ignored. The term 'active bars' implies bars which, under given hydrodynamic conditions, interact intensively with the surf zone wave field to produce breakers and specific, local water circulations.

The research was carried out at the Coastal Research Station (CRS) at Lubiatowo, Poland, located on the southern Baltic coast (see Figure 1). The non-tidal beach usually features four longshore sandbars and a gently

sloping seabed with $\beta = 0.015$. The seabed itself consists of fine quartz sand with a mean grain diameter $D_{50} \approx 0.22$ mm. The absence of tides leaves wind waves as the only driver of water motion in the nearshore zone. The complex seabed configuration with many bars produces multiple wave-breaking patterns and specific wave energy dissipation. Only a small fraction of the total wave energy (about 30% on average) reaches the direct proximity of the shoreline (Pruszak et al. 1999). Statistical analyses were performed mostly using the Discrete Wavelet Transform (DWT) method (Mallat 1989, Kumar & Foufoula-Georgiou 1997).

2. Field conditions and observations

The coastal section where the long-term observations and measurements were carried out is approximately 3 km long and usually has 3–5 more or less linear and stable longshore bars. The first stable inner bar $R_{(I)}$ appears about 100–120 m from the shoreline, the second inner bar $R_{(II)}$ about 220–250 m, while the third (offshore bar) $R_{(III)}$ is about 400–450 m offshore. The fourth and fifth bars are usually combined, forming one larger entity $R_{(IV)}$ about 650–850 m offshore. In this bar system the first and the fourth bars, R_I and R_{IV}, can be treated as the two extreme features (inner and outer bars), whereas the second (R_{II}) and the third (R_{III}) bars can be regarded as middle bars. All these four basic bars are

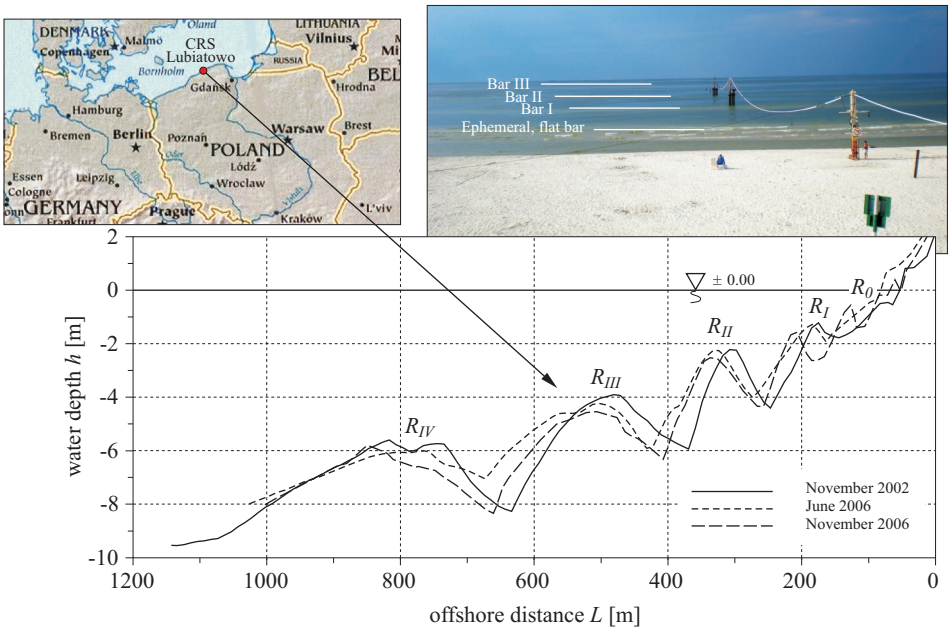

Figure 1. Study area at CRS Lubiatowo

characterised by a fairly high stability, that is, they do not dissipate but can change their locations and shapes only to a limited extent. Observations of the displacements of bar crests during severe storms indicate that the resulting migration is no greater than ten metres or so (Figure 1). Long-term studies on the coastal section under scrutiny indicate that the average rate of basic bar migration during winter is 0.3–0.6 m day^{-1} and is directed offshore. In summer onshore migration takes place at various rates between 0.07 and 0.21 m day^{-1} (Pruszak 1998). Apart from these fairly stable bars, an ephemeral, flat and shallow feature (an unstable bar or swash bar R_0) may be encountered near the shoreline, but it often migrates and disappears. Situated between the first stable longshore bar and the shoreline, this shallow bed form emerges several tens of metres offshore and definitely has some impact on the variability and characteristics of shoreline morphology. The presence and locations of bars in connection with instantaneous wave conditions determine the number and location of wave breakers. For ordinary, non-storm waves these occur over the first and possibly the second bar crests, i.e. 100–250 m offshore, where the water column is fairly shallow. Stronger (storm) waves can also break over the outer bars producing several more or less parallel lines of breakers. For small waves, breaking occurs over the shallow area close to the shoreline (R_0) or just in front of it, i.e. from several to several tens of metres offshore.

The underwater slope has a gentle average inclination of $\beta = 0.015$ with a maximum of 0.04 at the shoreline itself. The incoming deepwater waves undergo substantial transformation in the surf zone owing to the presence of bars. Multiple breakers dissipate the wave energy. During storms of medium strength, the deepwater significant wave height H_s, measured at a seabed depth of $h \approx 15$–20 m, can reach $H_s = 4.5$ m with the maximum values of $H \approx 7$ m. The corresponding wave period T in such conditions varies between 5 and 9 s. Close to the shoreline, for a water depth $h < 1$ m, the parameters of storm waves are strongly reduced (see Figure 2).

By making use of the surf-scaling parameter

$$\xi = \frac{\frac{H_z}{2}\,\omega^2}{g\,s^2} = \frac{2\pi^2 H_z}{gT^2 s^2}, \tag{4}$$

where H_z is the wave height at the breaking location, $\omega = 2\pi/T$ is the angular wave velocity, and $s = \tan\beta$ is the mean seabed slope, one can describe the scale of surf-zone dissipative processes. Assuming that the average breaking wave height range at CRS Lubiatowo lies between $H_z \cong 0.5$ and 1.0 m, with a corresponding period of $T \approx 4.5$ s, the value of ξ is $124 < \xi < 248$. Such values of the surf scaling parameter clearly indicate that the Lubiatowo beach is a highly dissipative coastal system

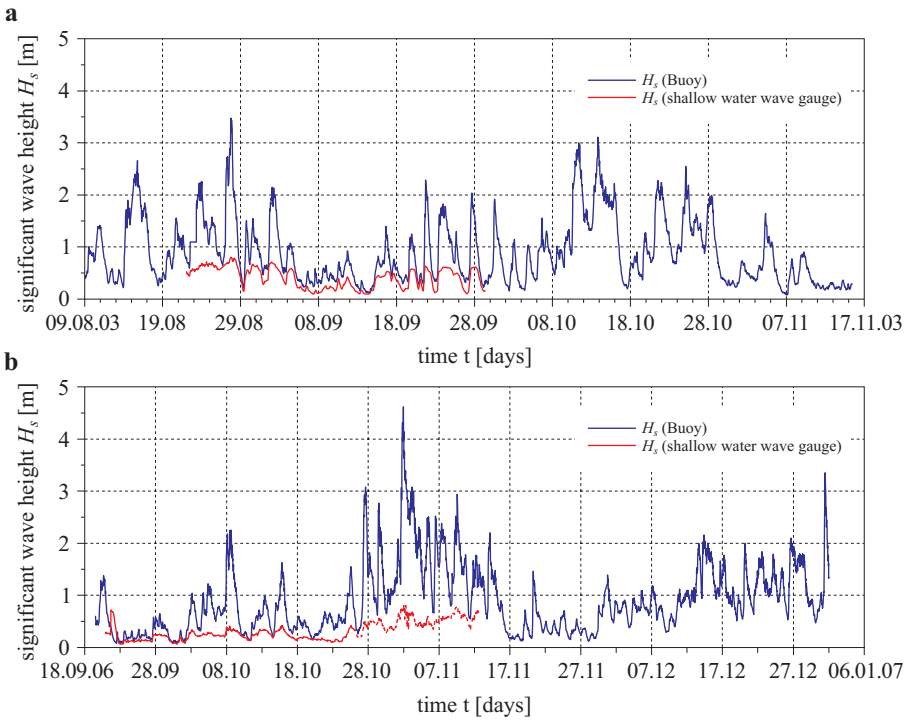

Figure 2. Deep-water and shallow-water (at depth $h \approx 0.5$–0.7 m) wave records measured in 2003 (a) and 2006 (b)

(Carter 1988, Komar 1998). This implies that it produces potentially worse conditions for the generation of edge waves and their influence on the formation of shoreline forms than are encountered on reflective beaches.

Massel & Musielak (1980) performed the first studies describing the generation of infragravity waves in the dissipative multibar system characteristic of the southern Baltic. Pruszak et al. (2007) presented a significantly more comprehensive analysis, focusing on the identification of infragravity waves in the southern Baltic region and the search for their possible relationships with rhythmic shoreline features. This analysis revealed the existence of two clearly perceptible infragravity components with periods of 30–40 s and 100–120 s. Separate investigations produced clues indicating that the mainly standing edge waves can be linked to smaller rhythmic shoreline features from several to a dozen or so metres in size. The 2006 field measurements, extended with respect to the 2003 field study, focused in particular on studies of larger rhythmic forms (mega-cusps), whose wavelengths cover the interval 500 m $> L_c >$ 20 m. One of the aims of that field campaign was to seek relationships between larger rhythmic forms and hypothetical sources of their generation. During both campaigns (2003

and 2006) a number of detailed shoreline configurations were measured covering sections from several hundred metres to several kilometres in length. The recorded shoreline configurations comprised waterline points $\mathrm{h}(\mathrm{x},\mathrm{y}) = 0$ obtained at given instantaneous seawater levels. These shoreline records were accompanied by measurements of waves, currents and wave breaking positions, observed in the associated time scale, before the records of shoreline morphology were completed. Deep-water waves were recorded at depths of $h \approx 20$ m (2003) and $h \approx 15$ m (2006) with a directional wave rider capable of measuring directional wave spectra. Wave parameters (height and period) in the shallow region were registered with a resistor wave gauge attached to a steel rod driven into the seabed with a water jet close to the shoreline at $h \approx 0.4$–0.7 m. Deep-water waves were measured continuously from 8 August to 15 November 2003 and from 12 September to 31 December 2006. Every wave parameter record contained hourly averaged quantities. Figures 2a and b show the deep- ($h \approx 15$–20 m) and shallow-water ($h < 1$ m) wave conditions measured in 2003 and 2006 respectively.

The nearshore morphology was characterised by the shoreline configuration and bar locations. In the period 2003–2006 more than 20 detailed shoreline configurations were recorded, covering sections between 0.5 and 7.5 km long and retaining their fine rhythmic features. The longshore spatial steps of shoreline measurements ranged from 2 to 50 m. The shoreline position of morphological sand forms was measured with an optical rangefinder and surveying rod, whose positions were determined using GPS equipment. The exact locations of the bars were determined at the same time. Table 1 (see page 196) sets out the measurements selected for DWT analysis.

3. Data analysis and results

3.1. Method (DWT)

In general the Discrete Wavelet Transform method (DWT) is capable of capturing slow, medium and fast oscillations in the time series representing random signals. Importantly, the analysed series can be divided into spectrally disjoint patterns describing its variability in low, medium and high frequency bands. Suitably chosen wavelet functions ensure that these patterns are orthogonal. Each wavelet represents a single waveform that can be dilated or contracted by means of a scale parameter λ while retaining two basic quantities:

1) the integral of each wavelet in the infinite $\pm\infty$ limits is equal to zero;

2) the integral of the square of each wavelet in these limits is equal to one; in general, dilated wavelets are used to identify slow-varying oscillations, whereas contracted ones are capable of extracting high-frequency oscillations.

In the discrete form we adopt the value $\lambda_0 > 1$, so that discrete scales can be written as $\lambda = \lambda_0^m$, where m is an integer. Moreover, the value $t_0 > 0$ allows discrete moments of time to be expressed in the form $t = nt_0\lambda_0^m$, where n is also an integer. The most convenient discretisation is possible for $\lambda_0 = 2$ and $t_0 = 1$, so that the discrete wavelet function $\psi_{m,n}$ can be written in the form (5)

$$\psi_{m,n}(u) = 2^{-m/2}\psi(2^{-m}u - n) = \frac{1}{\sqrt{2^m}}\psi\left(\frac{u - n2^m}{2^m}\right). \tag{5}$$

The choice of an orthogonal wavelet function guarantees that all its translates and dilates are orthogonal for all m and n (Mallat 1989), and each finite signal f, i.e. $\int_{-\infty}^{\infty} f^2(t)dt < \infty$, can be approximated to an arbitrary precision by means of the linear combination (6)

$$f(t) = \sum_{m=-\infty}^{\infty}\sum_{n=-\infty}^{\infty} D_{m,n}\,\psi_{m,n}, \tag{6}$$

where the external sum is over scales and the internal one over time. The coefficients $D_{m,n}$ are the values of the discrete wavelet transform for the scale m and time n:

$$D_{m,n} = \sum_{-\infty}^{\infty} f(u)\psi_{m,n}(u)du. \tag{7}$$

Signal decomposition using DWT is called multi-resolution analysis: the signal components contain only low, medium or high frequency oscillations. Let $f_m(t)$ denote the signal $f(t)$ approximated by points every 2^m units. When m decreases, the scale also decreases and the resolution increases. The quantity $f_m(t)$ is called the smooth representation of the signal $f(t)$ for the scale m. A one-step greater resolution is obtained when the detailed $f'_m(t)$ is added:

$$f_{m-1}(t) = f_m(t) + f'_m(t). \tag{8}$$

The smooth representation for the scale m can be determined with eq. (6),

$$f_m(t) = \sum_{n=-\infty}^{\infty} C_{m,n}\,\phi_{m,n}(t), \tag{9}$$

where

$$\phi_{m,n}(t) = 2^{-m/2}\phi(2^{-m}t - n). \tag{10}$$

Function $\phi(t)$, the scaling function, is determined unequivocally by the chosen wavelet function. The coefficients $C_{m,n} = \int_{-\infty}^{\infty} \phi_{m,n}(u)f(u)du$ are approximate values of the signal $f(t)$ for the scale (resolution) m and time n. The detail $f'_m(t)$ is computed using the quantities $D_{m,n}$:

$$f'_m(t) = \sum_{n=-\infty}^{\infty} D_{m,n}\,\psi_{m,n}. \tag{11}$$

Figure 3 presents the nearly symmetric and orthogonal wavelet function used in the analysis (known as 'coif2' in the literature). Since there are many other similar functions, the DWT results are not identical but dependent upon the choice of wavelet. For diagnostic purposes, however, they are similar enough, which allows the background processes accounting for slow, medium or high frequency oscillations to be determined. The authors recommend that less advanced wavelets be used for short signals; the longer the signal, the more complex the wavelet that can be applied, but symmetric wavelets are preferable in all cases.

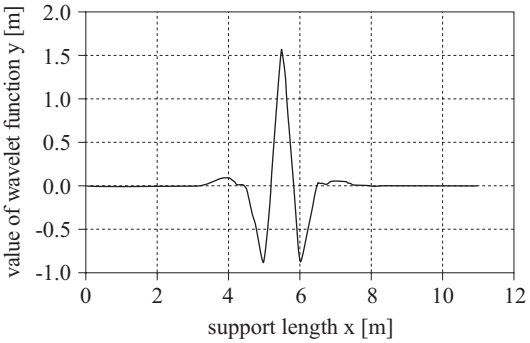

Figure 3. The single near-symmetric and orthogonal wavelet function used in this analysis

3.2. Analysis

The observed multi-scale rhythmic shoreline forms are due to numerous, often complex, hydrodynamic factors and to the seabed configuration. When the wave field can operate for a sufficiently long time, apart from the more or less stable sequences of shorter mega-cusps in the range of several tens of metres or so, a longer undulation can develop with wavelengths

Figure 4. Longshore structure of shoreline rhythmicity patterns (L_c – cusp wavelength, A_c – cusp indentation length)

ranging up to hundreds of metres (Carter 1988, Komar 1998, Pruszak et al. 2007). Figure 4 illustrates the spatial distributions of the most frequently observed more or less regular undulations (beach mega-cusps with wavelength L_c and indentation length A_c) under southern Baltic conditions.

The Discrete Wavelet Transform (DWT) was employed to identify the statistical parameters of shoreline rhythmicity embedded in the records of shoreline configurations. Importantly, DWT is capable of dividing these records into patterns describing short, medium and long undulations, which in the temporal domain correspond to short, medium and long periods, or equivalently, high, medium and low frequencies. The shortest undulations that can be extracted with DWT must obey the Nyquist principle. For example, if the sampling step $\Delta x = 8.5$ m, the finest filter ('window') can capture the features with a cusp wavelength L_c between 17 and 34 m. The lower/upper limit of the next window is equal to twice the lower/upper limit of the previous one. In our example, the next window contains features in the range between 34 and 68 m.

To illustrate the analyses done for all records, four cases are presented, featuring various window lengths (see Figure 5). The case of 11 November 2006 (Figure 5a) revealed fine undulations containing 16–64 m long cusps with a peak value $L_c^p = 27$ m. This record had a sampling interval of roughly 4 m, so the resulting windows (filters) were 8–16 m, 16–32 m,

32–64 m, etc. Thus, the cusps between 16–64 m are the summed 16–32 m and 32–64 m filters. The peak band, where spectral estimates are at least 60% of the peak value, indicates that most cusps are concentrated between 24 and 40 m. An earlier analysis of 2 September 2006 (Figure 5b) indicated longer cusps in the 32–128 m range. Since the sampling interval was the same as before, it shows that the cusps are present in the three summed filters, i.e. 16–32 m, 32–64 m and 64–128 m. The peak value $L_c^p = 80$ m and the corresponding peak band identifies most cusps in the range between 65 and 120 m. The next example dates from 30 November 2006 (Figure 5c) and features the finest sampling step of 3.6 m. Here, relatively long cusps were identified, with $L_c^p = 180$ m. They occupy the summed filters between 57.6 and 230.4 m; the peak band is located between 130–220 m. Finally, one of the first records, dating back to 12 November 2003 (Figure 5d), displayed quite long mega-cusps. Here, the record was obtained along a nearly 8 km long coastline with a rather coarse sampling step of 41 m. For this record a value of $L_c^p = 340$ m was found, situated in the peak band between 240–380 m within the summed filters in the range 164–656 m. Figure 5 shows these example analyses, which are representative of the whole study.

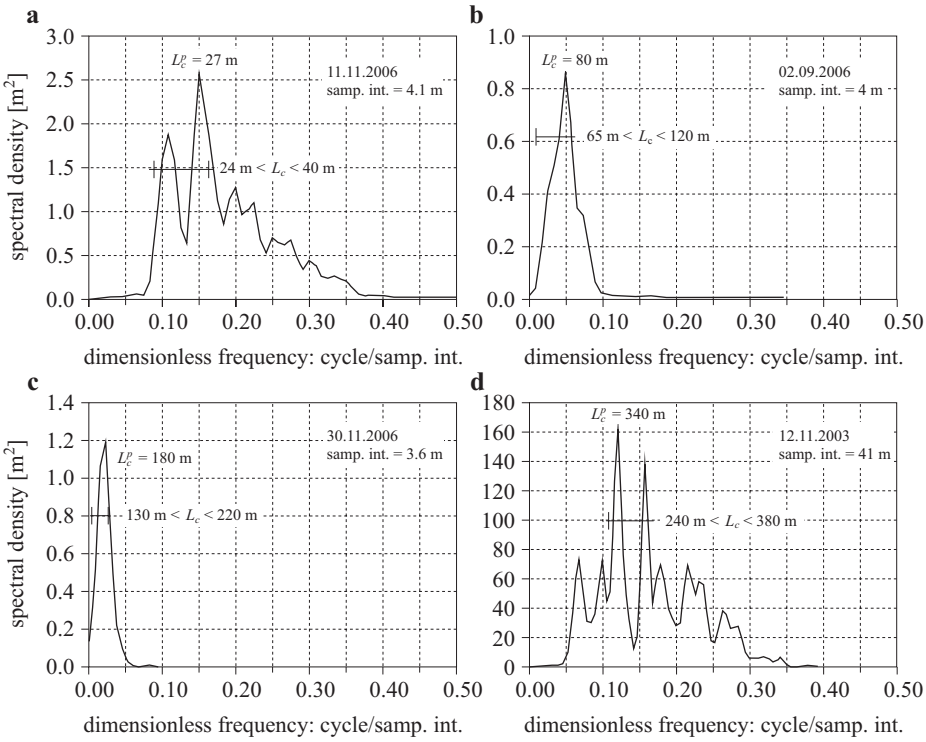

Figure 5. Spectra of shoreline wavelengths for four different filters (a, b, c, d)

The incorporation of not only the peak value of L_c^p, but also a certain range of its variability (peak band), provides a more representative description of mega-cusps generated under natural, random conditions. Among other things, this is because the exact geometry of rhythmic shoreline forms is related to the continuous adaptation of the shoreline to dynamically varying hydrodynamic conditions in the adopted (associated) time scales prior to shoreline measurement(s). The working assumption was that the peak band covers the interval where the spectrum values are $> 60\%$ of the L_c^p peak wavelength.

As can be seen from the DWT analysis performed for cusps with wavelengths in the interval 20 m $< L_c <$ 500 m, the majority of cusps lie between 25 and 250 m (see Table 1). These wavelengths correspond to offshore distances from the shoreline to the ephemeral bar R_0, and also to the inner (R_I) and middle bar (R_{II}). At the same time, it should be pointed out that in the whole multi-bar system, it is precisely these bars that are the best correlated with shoreline changes (see Pruszak et al. 1999). The offshore bars R_{III} and R_{IV} are more weakly correlated with shoreline positions, which could be one of the reasons for the rare occurrence of cusps with wavelengths $L_c >$ 250–500 m. Furthermore, field observations of the stability of rhythmic shoreline forms indicate that greater wavelengths are usually characterised by their low longshore and cross-shore regularity.

Field observations and comparisons of offshore breaker locations in the associated time scale prior to shoreline measurement, corresponding to the positions of bars R_i (mainly inner bars), with the simultaneously present mega-cusps of length L_c suggest that they are convergent. It can therefore be assumed that, apart from the previously indicated correlation between the variations of bars (R_0, R_I, R_{II}) and shoreline (Pruszak et al. 1999), there is also a physical relationship between the dimensions of beach mega-cusps and the currently active bar locations (their distance to the shoreline). Such a hypothesis derives from the supposition that large-scale self-regulation processes in a dissipative multi-bar beach system are linked to the mechanisms of formation of water motion and 3D current circulations (circulation cells) at various scales. Assuming further that the spatial dimensions of circulation cells at various scales are linked to the local nearshore zone seabed configuration (morphological forms), one should expect a correlation between the wavelengths of mega-cusps, determined by the longshore dimensions of circulation cells, and their cross-shore dimensions related to the locations of consecutive bars. The largest circulation cells can be formed with spatial dimensions that can match the distance from the shoreline to the most active offshore bars. The actual number of circulation cells interacting with the shoreline depends on the

Table 1. Rhythmic shoreline wavelengths and bar positions following statistical analysis

No.	Date	Mega-cusp wavelength L_c [m]				Length of measured shoreline section/ Sampling interval (step) [m]/[m]	Max. breaker zone width/ Period of assumed wave situation before morphological measurements [m]/[d]	Offshore distances of active bars R_i [m]
		20–70	75–175	180–350	350–500			
1	2	3	4	5	6	7	8	9
1	03.09. 2003		85; 120	250		2400/10	∼450 01–03.09. 2003	$R_0 \sim 60$; $R_I \sim 120$ $R_{II} \sim 250$
2	03.10. 2003	20; 50	125			2400/8.5	∼350 30.09–02.10. 2003	$R_0 \sim 40$; $R_I \sim 120$ $R_{II} \sim 250$
3	07.10. 2003	25; 70	125			800/5	∼250 05–07.10. 2003	$R_0 \sim 30$; $R_I \sim 120$ $R_{II} \sim 250$
4	19.10. 2003			280		7500/50	350 11–18.10. 2003	$R_0 \sim 30$; $R_I \sim 120$ $R_{II} \sim 250$
5	27.10. 2003	30				500/8.5	∼450 25–27.10. 2003	$R_0 \sim 40$; $R_I \sim 120$ $R_{II} \sim 250$
6	12.11. 2003			185; 340		75800/40	∼320 09–11.11. 2003	$R_I \sim 120$; $R_{II} \sim 250$
7	26.11. 2003	70		240		2500/9.5	∼250 24–26.11. 2003	$R_I \sim 120$; $R_{II} \sim 250$
8	06.01. 2006		90	200		500/4	∼230 04–06.01. 2006	$R_I \sim 100$; $R_{II} \sim 220$
9	04.04. 206	48	110			1200/10	∼110 01–03.04. 2006	$R_0 \sim 40$; $R_I \sim 100$

Table 1. (*continued*)

1	2	3	4	5	6	7	8	9
10	02.05. 2006	No distinct shoreline rhythmicity				500/4	∼ 25 01–02.05. 2006	$R_0 \sim 25$
11	02.06. 2006	34–80				500/4	110 30.05–01.06. 2006	$R_0 \sim 30$; $R_I \sim 100$
12	29.06. 2006	30	100			500/4	110 27–29.06. 2006	$R_0 \sim 30$; $R_I \sim 100$
13	21.07. 2006		115			500/10	∼110 18–20.07. 2006	$R_I \sim 100$
14	02.09. 2006		80–85			2500/4	∼110 31.08–2.09. 2006	$R_I \sim 100$
15	26.09. 2006	30				600/4	∼30 23–26.09. 2006	$R_0 \sim 30$
16	19.10. 2006	35–50	100–125			600/4	∼110 17–19.10. 2006	$R_0 \sim 25$; $R_I \sim 100$
17	26.10. 2006	20–25; 50	90			525/4	∼250 24–26.10. 2006	$R_0 \sim 40$; $R_I \sim 120$ $R_{II} \sim 250$
18	11.11. 2006	25–30	115			500/4	∼450 09–11.11. 2006	$R_0 \sim 25$; $R_I \sim 100$ $R_{II} \sim 220$
19	30.11. 2006	20–25		180		500/4	∼250 26–29.11. 2006	$R_0 \sim 25$; $R_I \sim 100$ $R_{II} \sim 220$

R_i – offshore distance of 'active' bar to shoreline position.

number of active bars and the hydrodynamic conditions reflecting the wave climate. Proportionately to the number of 3D circulation cells, one should expect the same number of closest corresponding sets (pairs) of shoreline wavelengths and offshore distances of the successive bars. As in the case of

the correlations between the simultaneous variability of bar locations and shoreline, one can expect that the significance of potential correlations will decrease with increasing offshore distance.

It is quite clear that in the majority of the 19 data sets presented in Table 1 there are several pairs L_c and R_i of cusp lengths and distances to active bars. In the light of the above discussion, the quantities L_c in all these cases were linked with dimensionally the most similar counterparts R_i. For example, 3 pairs ($L_c = 85$ m – $R_i = 60$ m, $L_c = 120$ m – $R_i = 120$ m and $L_c = 250$ m – $R_i = 250$ m) were associated with set 1, another 3 pairs ($L_c = 20$ m – $R_i = 40$ m, $L_c = 50$ m – $R_i = 40$ m and $L_c = 125$ m – $R_i = 120$ m) with set 2, and 2 pairs with the most divergent values ($L_c = 185$ m – $R_i = 120$ m and $L_c = 340$ m – $R_i = 250$ m) with set 6. Figure 6 is a graphical representation of eq. (12).

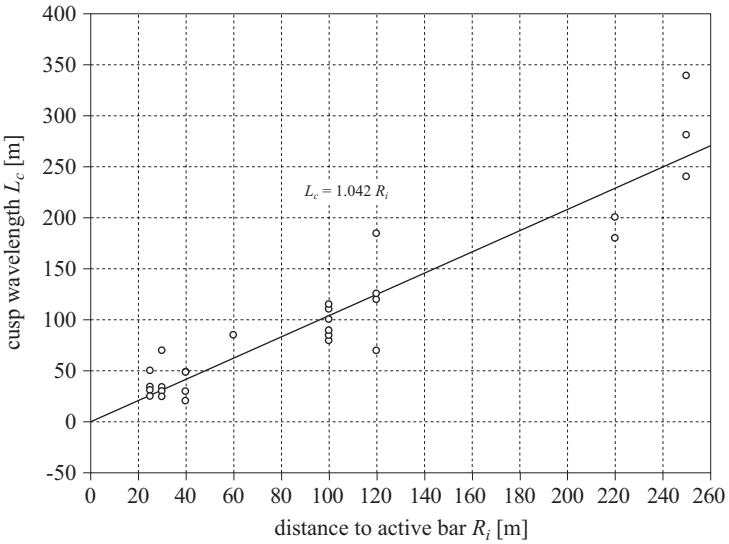

Figure 6. Correlation between mega-cusp wavelength L_c and the offshore distance of an 'active' bar to the shoreline position R_i

Mathematically, this empirical relationship can be expressed by eq. (12), which relates cusp length L_c to distance R_i (see Table 1), with a correlation coefficient $r = 0.92$.

$$L_c = 1.04 R_i. \tag{12}$$

The above relationship could be assumed to be a first confirmation and rough verification of the hypothesis that the existence and spatial arrangement of bars is an important component of surf zone self-regulation processes, which influences/generates shoreline undulations with a given

rhythmicity (mega-cusp lengths). In this context, surf zone self-regulation processes should be understood as mutual interactions and couplings between the inner bars and greater shoreline rhythmic forms. The couplings between the bars and large mega-cusps demonstrate the fairly large-scale character (surf zone) of the self-regulation processes, while smaller cusps with wavelengths of several to a dozen metres or so are limited only to swash zone self-regulation processes (see Coco 1999).

The different inertias of hydro- and morphodynamic processes give rise to a time lag before a new mega-cusp structure is formed in response to the sufficient duration and intensity of given wave climate conditions. Long-term observations of rhythmic shoreline forms at CRS Lubiatowo indicate that, apart from the hydrodynamic conditions, the time of formation and the stability of cusps also depend on the dimensions (scale) of these forms. Smaller rhythmic shore undulations with wavelengths of several metres, $L_c \approx 5$–20 m, are temporally highly variable and rather unstable, and are most frequently the result of the instantaneous wave climate. As cusp dimensions increase, so do their formation time and their stability. Therefore, the particular structure of the recorded mega-cusps is not the result of instantaneous hydrodynamic conditions but derives from their averaged representation over the associated time scale before the measurement of shoreline rhythmicity. This time scale may include the development/duration/recession of a storm, or given, often very individual, intensive wave climate conditions. In such situations it is difficult to determine explicitly the time scale of formation and stability of each mega-cusp. On the basis of the authors' own observations of these forms in situ, the variability of longshore bars and of the shoreline configuration with its small bay-type mega-forms, as well as the results of other studies (e.g. Wright & Short 1984), it can be assumed that, on average, this time scale will be in the range of a dozen or so to several tens of hours.

As a result of the different intensity and variability of wind waves and wave-driven currents, the indentation length of shoreline rhythmicity A_c can take different dimensions. Figure 7 illustrates the variability in A_c for four examples of shoreline rhythmicity.

Based on the range of variability of L_c (see Table 1), the corresponding values of A_c and L_c derived from statistical analyses are set out in Table 2, which also contains average $(L_c/A_c)_{av}$ ratios derived from L_{av} and A_{av} of the relevant ranges of these quantities.

Figure 8 illustrates the empirical relationship between the relevant values of L_c and A_c. A good fit to the observations with a coefficient of determination $R^2 = 0.904$ was achieved for the following linear expression:

$$L_c = f(A_c) \approx 57.22 A_c. \tag{13}$$

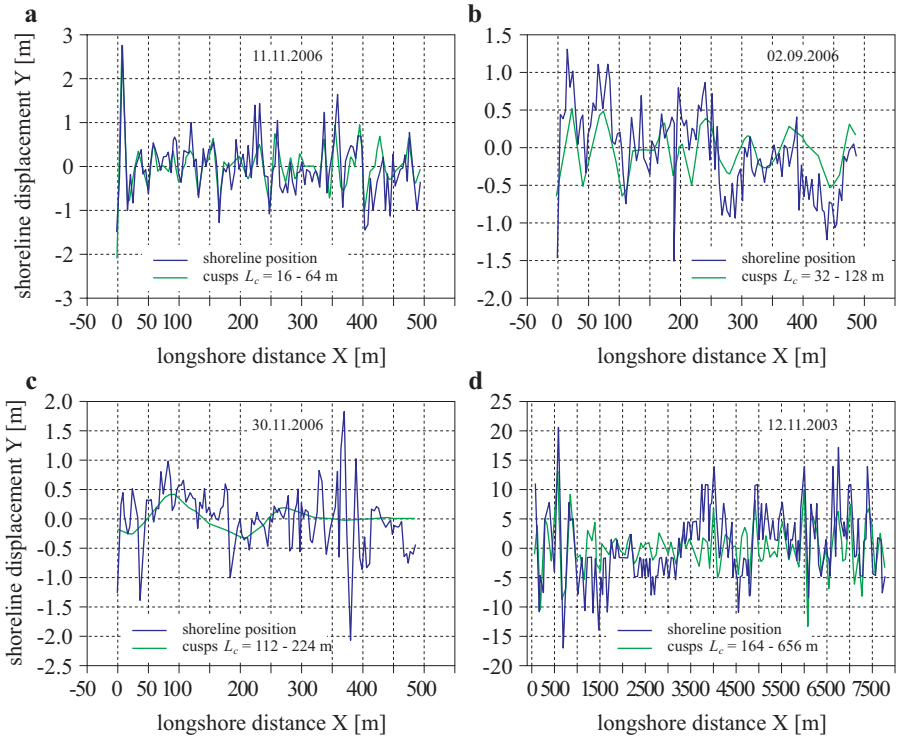

Figure 7. Longshore variability of mega-cusp indentation length A_c for four different L_c filters ('windows') (bands of mega-cusp wavelength) (a, b, c, d)

Table 2. Ranges of variability of mega-cusp wavelengths L_c and indentation length A_c

Length L_c [m]	Indentation length A_c [m]	$(L_c/A_c)_{av}$
350–500	2.5–9	75
180–350	2–7	60
75–175	1.5–3.5	50
30–70	1–2.5	30
20–30	1–2	17

Figure 8 and eq. (13) thus demonstrate the linear character of the relationship between L_c and A_c. Hence, the average ratio L_c/A_c can vary from 75 for long undulations to only 20 for short mega-cusps with a length in the 15–20 m range. Comparing the values of L_c/A_c from tidal, reflective oceanic shores, where cusp length may lie between 3 m $< L_c <$ 90 m (max 130 m) (see Nolan et al. 1999), with the southern Baltic

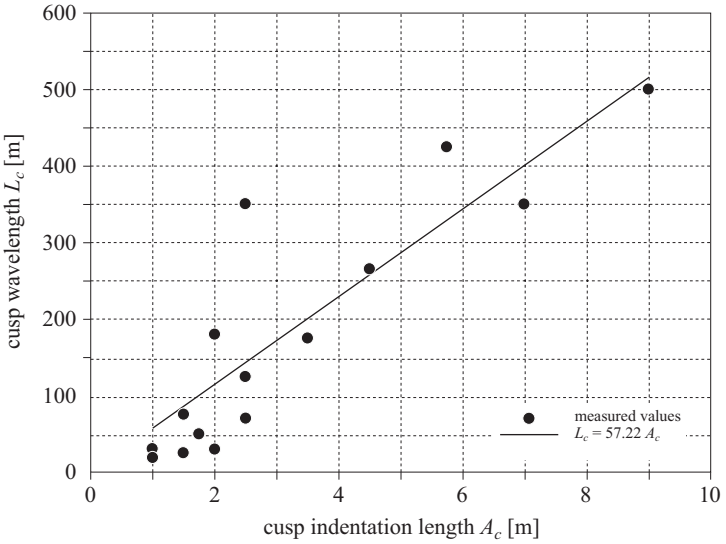

Figure 8. Empirical relationship between cusp wavelengths L_c and cusp indentation length A_c

coast, where cusp lengths are typically 20 m $< L_c <$ 500 m, we can see that these ratios are one order of magnitude greater in the former case. This means that non-tidal (microtidal) conditions and dissipative beaches generate strongly flattened and less vivid rhythmic shore undulations $[(L_c/A_c)_{\text{this study}}/(L_c/A_c)_{\text{Nolan et al.}} \approx 25]$ than the conditions of mesotidal and reflective beaches.

4. Conclusions

The study has confirmed that bars and their contribution to wave energy dissipation play a key role in the morphodynamic processes occurring in the surf zone of the study area. In such a physical system the bars and longshore dimensions of larger rhythmic shoreline forms are interrelated and govern one another; this tallies with previous results (Wright & Short 1984).

Field observations, and comparison of the wavelengths of larger rhythmic shoreline features (mega-cusps) with the offshore distances of 'active' bars, suggest that these quantities are convergent. The results of empirical analyses can be treated as tentative confirmation of the hypothesis regarding the importance of the part played by bars (mainly the inner ones) in the formation of the longshore geometry of shoreline rhythmicity.

Since the formation and evolution of large mega-cusps are characterised by a much greater inertia than the highly variable hydrodynamic conditions, it should be assumed that the measured rhythmic shoreline mega-forms

are due to wave action (triggering bar activity) at time scales of many hours. In the light of numerous observations, it can be established that the approximate time scale of the hydrodynamic conditions required for the formation/reconfiguration of large cusps is of the order of a stronger single storm, or a sequence of weaker storms, or distinctly stable wave conditions.

The relationship between the wavelengths of mega-cusps with the offshore distances of 'active' bars could be associated with the large-scale (spanning most of the surf zone) self-regulation of a dissipative multi-bar beach system. This process is linked to the mechanisms of formation of various kinds of water motion and multi-scale 3D current circulations, specific to the section of coast in question. The constant tendency towards equilibrium between hydrodynamic forcing (different circulations and structures) and shoreline-seabed response is an additional factor here.

According to the study results, the indentation of an individual rhythmic form in the dissipative coastal systems of the southern Baltic varies from several tens of centimetres to several metres, depending on its wavelength. The indentation to wavelength ratio of mega-cusps for the studied dissipative environment may be one order of magnitude smaller than that identified by Nolan et al. (1999) for cusps and smaller mega-cusps on oceanic beaches. This means that dissipative beaches with non-tidal or microtidal conditions generate rhythmic, flattened shore undulations with much smaller indentations than is the case on mesotidal and reflective beaches. Moreover, the distinctiveness and regularity of beach rhythmicity is much more pronounced on reflective, tidal ocean beaches than on the non-tidal dissipative beaches of shelf seas.

Owing to the limited data and the assumptions made in the analyses presented here, the results are of a preliminary nature and as a whole require further research and field studies.

References

Carter R. W. G., 1988, *Coastal environments*, Acad. Press, London, 617 pp.

Coco G., Huntley D., O'Hare T. J., 1999, *Beach cusp formation: analysis of a self-organisation model*, [in:] *Coastal Sediments '99*, N. C. Kraus & W. G. McDougal (eds.), ASCE, Reston, 2190–2205.

Coco G., Huntley D., O'Hare T. J., 2001, *Regularity and randomness in the formation of beach cusps*, Mar. Geol., 178 (1), 1–9.

Guza R. T., Inman D., 1975, *Edge waves and beach cusps*, J. Geophys. Res., 80 (21), 2997–3012.

Komar P. D., 1998, *Beach processes and sedimentation*, (2nd edn.), Prentice Hall, Upper Saddle River, NJ, 544 pp.

Kumar P., Foufoula-Georgiou E., 1997, *Wavelet analysis for geophysical applications*, Rev. Geophys., 35 (4), 385–412.

Mallat S. G., 1989, *A theory for multiresolution signal decomposition: The wavelet representation*, IEEE T. Pattern. Anal., 11 (7), 674–693.

Massel S. R., Musielak S., 1980, *Long-period oscillations in the surf zone*, Rozpr. Hydrotechn., 41, 79–84.

Nolan T. J., Kirk R., Shulmeister J., 1999, *Beach cusp morphology on sand and mixed sand and gravel beaches, South Island, New Zealand*, Mar. Geol., 157 (3), 185–198.

Pruszak Z., 1998, *Dynamics of beaches and sand beds*, Wyd. IBW PAN, Gdańsk, 463 pp., (in Polish).

Pruszak Z., Różyński G., Szmytkiewicz M., Skaja M., 1999, *Quasi seasonal morphological shore evolution response to variable wave climate*, [in:] *Coastal Sediments '99*, N. C. Kraus & W. G. McDougal (eds.), ASCE, Reston, 1081–1093.

Pruszak Z., Różyński G., Szmytkiewicz M., Skaja M., 2007, *Field observation of edge waves and beach cusps on the Baltic Sea coast*, J. Coastal Res., 23 (4), 846–860.

Pruszak Z., Różyński G., Zeidler R. B., 1997, *Statistical properties of multiple bars*, Coast. Eng., 31 (1–4), 263–280.

Ruessink B. G., 1998, *Infragravity waves in a dissipative multiple bar system*, Ph. D. thesis, Univ. Utrecht, Netherlands, 245 pp.

Sunamura T., 2004, *A predictive relationship for the spacing of beach cusps in nature*, Coast. Eng., 51 (8–9), 697–711.

Werner B. T., Fink T. M., 1993, *Beach cusps as self-organised patterns*, Sciences, 260 (5110), 968–971.

Wright L. D., Short A. D., 1984, *Morphodynamic variability of surf zones and beaches: a synthesis*, Mar. Geol., 56 (1–4), 93–118.